ISSN 1068–3372, Journal of Contemporary Physics (Armenian Academy of Sciences), 2017, Vol. 52, No. 2, pp. 110–120. © Allerton Press, Inc., 2017.
Original Russian Text © M.A. Aginian, S.G. Arutunian, D. Cho, M. Chung, G.S. Harutyunyan, S.-Y. Kim, E. G. Lazareva, A.V. Margaryan, 2017, published in Izvestiya Natsional'noi Akademii Nauk Armenii, Fizika, 2017, Vol. 52, No. 2, pp. 151–165.

# Precise Out-Vacuum Proton Beam Monitoring System Based on Vibrating Wire

**M. A. Aginian[a], S. G. Arutunian[a], D. Cho[b], M. Chung[b], G. S. Harutyunyan[a], S.-Y. Kim[b], E. G. Lazareva[a*], and A. V. Margaryan[a]**

[a] *Alikhanyan National Scientific Laboratory, Yerevan, Armenia*
[b] *Ulsan National Institute of Science and Technology, Ulsan, Korea*
[*] *ella.lazareva@yerphi.am*

Received January 9, 2017

**Abstract**—As an instrument for Korea Multi-purpose Accelerator Complex (KOMAC) facility proton beam profiling, a vibrating wire monitor (VWM) has been installed and tested at TR23 target room. Experiments were done at very low (100 nA) beam current conditions. At the number of particles about $10^{11}$ proton/train and trains repetition rate of 0.1 Hz we have measured the beam profile by a few scanning steps. The experience accumulated in these experiments turned out to be useful for the VWM upgrades (e. g. understanding interactions of protons with wire materials and heat transfer processes) and will be particularly helpful for the KOMAC beam halo measurements in the future high-current operation.

**DOI:** 10.3103/S1068337217020049
*Keywords*: KOMAC, proton beam, vibrating wire monitor

## 1. INTRODUCTION

The vibrating wire monitor (VWM) with large aperture size [1] has been used for proton beam profile measurements. The principle of operation of this device, the following [2]: under the exposure to the beam, the initially tensioned wire is heated by the beam particles, which leads to the decrease of the wire tension. If the wire is vibrating on its natural frequency, such tension change affects the frequency value. Precise measurements of the frequency allow to obtain information on how much particles are falling on the wire. By changing the wire position relative to the beam one can measure the beam profile. The wire oscillations in the VWM are generated by the interaction between the current passing through the wire and permanent magnetic field. Mechanical fluctuation in the wire generates electromotive force that is amplified and applied as a current backward. This process amplifies the mechanical movement. Due the high quality factor of the wire at the wire resonance, only oscillations at the wire natural frequency would 'survive'. As a result the wire starts to vibrate on the natural frequency. The electronic unit for oscillation generation, which has been developed in Yerevan Physics Institute, provides very stable oscillations of the wire. Microcontroller and precise quartz generator measure the frequency with accuracy better than 0.01 Hz for the measurement interval of 1 s.

The equilibrium temperature of the vibrating wire after the beam interaction depends on the monitor parameters as well as on the parameters of heat transfer from the beam particles to the wire material. The conditions in which the vibration occurs (vibrating wire can be placed either in vacuum or in the gas atmosphere) also affect the heat sink process, and therefore can influence the equilibrium temperature of

the wire. The absolute measurements of the beam particle flux require well defined information of all these parameters. Normalization by known total beam current would also be helpful.

High resolution of the VWM gives possibility to provide measurements even outside of the vacuum chamber, which significantly simplifies the measurement infrastructure (e. g., does not require a special vacuum chamber with feed mechanism, high vacuum feedthroughs etc. [3]).

In the presents work experimental results of the transverse beam profile measurements in the Korea Multi-purpose Accelerator Complex (KOMAC) [4–5] with maximum proton beam energy of 20 MeV are shown. Measurements were done in air at distance about 1 m from the vacuum chamber outlet where the beam energy was about 16 MeV. Detailed analysis on the losses in material taking into account the maximum energy transfer in a single collision (the Bethe–Bloch formula), as well as density and effect on the electrons *K* and *L*-shells corrections are also presented. The proton energy range of 10–10000 MeV for the tungsten wire are used in this experiment. This analysis allows to adjust the values of convection factor and coefficient of heat transfer from beam particle by using the experimental results of frequency shifts.

## 2. INTERACTION OF THE PROTON BEAM WITH WIRE

The beam penetrating the wire loses some energy with heating the wire. The wire temperature increased relative to the initial temperature can be calculated by the equation of balance between the power deposited into the wire and heat sink through the all possible thermal mechanisms: conduction along the wire to the end clips, convection losses to ambient atmosphere (in case if air is present), and losses through the radiation to ambient space. It is assumed that there are no other heat sources except the beam impact, and that profile of the balanced temperature has a triangle profile. The balance equation is written as

$$W_{\text{beam}} = W_{\lambda} + W_{\text{rad}} + W_{\text{conv}}, \tag{1}$$

where

$$W_{\lambda} = 2(T - T_0)\lambda \frac{S}{L/2} \tag{2}$$

− is the convection heat sink,

$$W_{\text{rad}} = \varepsilon\sigma_{\text{ST-B}} T_{\text{mean}}^4 \pi dL - \varepsilon\sigma_{\text{ST-B}} T_0^4 \pi dL \approx 2\varepsilon\sigma_{\text{ST-B}} T_0^3 (T - T_0)\pi dL \tag{3}$$

− is the heat sink through the radiation,

$$W_{\text{conv}} = \eta \frac{T - T_0}{2} \alpha_{\text{conv}} \pi dL \tag{4}$$

− is the convection heat sink.

Here $T_0$ is the ambient temperature, $T$ the maximal temperature increase (top of the temperature profile), $T_{\text{mean}} = (T + T_0) / 2$ the wires mean temperature, $d$ and $L$ diameter and length of the wire, $S$ the wires cross section, $\lambda$ the thermal conductivity of wires material, $\sigma_{\text{ST-B}}$ the Stefan–Boltzmann constant, $\varepsilon$ the radiation coefficient of the wire, $\alpha_{\text{conv}}$ the convection heat transfer coefficient, $\eta = 1$ if the wire is placed in atmosphere, and $\eta = 0$ if the wire is placed in vacuum.

Introducing $\Delta T = (T - T_0) / 2$ (mean overheating of the wire) we can find the following relation between $\Delta T$ and $W_{\text{beam}}$:

$$\Delta T = \frac{W_{\text{beam}}}{8\lambda S / L + 4\varepsilon\sigma_{\text{ST-B}} T_0^3 \pi dL + \eta\alpha_{\text{conv}} \pi dL}. \quad (5)$$

For parameter $\alpha_{\text{conv}}$ we use the equation for convection of cylinder by air with speed of $v$ [6]

$$\alpha_{\text{conv}} = 4.13 \frac{v^{0.8}}{d^{0.2}}. \quad (6)$$

For example, for the wire with length $L$ = 80 mm and oscillation frequency ~2000 Hz at the first harmonic we find $v \approx 0.3$ m/s (oscillation amplitude is about twice the wire diameter) and correspondingly $\alpha_{\text{conv}} \sim 17$ W/(m$^2$K). It follows that at room temperature the air convection is always dominant compared to the radiation sink.

In order to determine the parameter $W_{\text{beam}}$ should be calculated how much energy of the proton beam loses in the wire material. The proton by passing through the substance interacts with the electrons and nuclei present in the material by means of the electromagnetic force (ionization losses). Besides proton can also undergo a nuclear interaction and radiation processes. However, due to the large mass of the proton these effects are negligible compared to the ionization losses in the range of proton energies less than 5000 GeV [7]. Equation for specific ionization losses $dE/dx$ of a particle with mass $M >> m_e$ ($m_e$ is the electron mass) and velocity $v$ is known as the Bethe−Bloch formula [8], which is the basic expression used for energy loss calculations:

$$-\frac{dE}{dx} = 2\pi N_A r_e^2 m_e c^2 \rho \frac{Z}{A} \frac{z^2}{\beta^2} \left[ \ln\left( \frac{2m_e c^2 \gamma^2 \beta^2 W_{\max}}{\Phi^2} \right) - 2\beta^2 - \delta - 2\frac{C}{z} \right], \quad (7)$$

where $2\pi N_A r_e^2 m_e c^2 = 0.1535$ MeV cm$^2$/mol, $N_A$ = 6.022 × 10$^{23}$ mol$^{-1}$ is the Avogadro number, $r_e$ = 2.817 × 10$^{-13}$ the classical electron radius, $m_e c^2$ = 0.511 MeV, $\rho$ the density of absorbing material in g/cm$^3$, $Z$ the atomic number of absorbing material, $z$ the charge of incident particle in units of electron charge, $A$ the atomic weight of absorbing material in g/mol, $\Phi$ the mean ionization potential in eV, $\beta = v / c$, $\gamma = 1/\sqrt{1-\beta^2}$, $c$ the speed of light, $\delta$ the amendment, which takes into account the effect of medium density, $C$ the correction effect of the electrons binding on $K$- and $L$-shells, and $W_{\max}$ the maximal energy transfer in a single collision. The maximal energy transfer in the case of proton mass $m_p >> m_e$ is $W_{\max} \approx 2m_e c^2 \gamma^2 \beta^2$ (see, e. g. [8, 9]). For electrons and positrons the Bethe−Bloch formula differs from the equation (7).

In Table 1 some typical values for the proton ionization losses in tungsten ($Z$ = 74, $A$ = 183.84 g/mol = 19.3 g/cm$^3$) are presented without corrections in two energy ranges of protons. To obtain the mean value of the ionization potential of atoms of the absorbing material the value $I$ = 727 eV for $W_{\max}$, derived from direct experimental data [10], are used instead of the semi-empirical formula presented in [8].

For one proton, the energy loss $\delta_p$ in the wire can be roughly approximated as

$$\delta_p = \left( \frac{dE_p}{dx} \right) \times (\pi d / 4). \quad (8)$$

Some of the proton energy losses will be transferred to the heat in the wire material. The ratio of this transformation depends on proton energy, parameters of the wire materials and the wire geometry. In [11] a simulation was done to calculate the part of the interaction energy (actually ionization losses) deposited in the wire as heat. The carbon wire for a scanner [12] was chosen as a subject of investigation. Authors

**Table 1.** Ionization losses $dE_p/dx$ for a proton in the tungsten ( $E_p$ is the kinetic energy of proton)

| $E_p$, MeV | $dE_p/dx$, MeV/cm | $E_p$, MeV | $dE_p/dx$, MeV/cm |
|---|---|---|---|
| 10 | 384.63 | 1000 | 23.87 |
| 11 | 359.92 | 2000 | 22.63 |
| 12 | 338.57 | 3000 | 23.04 |
| 13 | 319.92 | 4000 | 23.66 |
| 14 | 303.46 | 5000 | 24.29 |
| 15 | 288.83 | 6000 | 24.88 |
| 16 | 275.73 | 7000 | 25.43 |
| 17 | 263.91 | 8000 | 25.92 |
| 18 | 253.20 | 9000 | 26.37 |
| 19 | 243.44 | 10000 | 26.79 |
| 20 | 234.50 | | |
| 21 | 226.29 | | |
| 22 | 218.71 | | |
| 23 | 211.70 | | |
| 24 | 205.18 | | |
| 25 | 199.11 | | |

of [11] estimated that for 100 MeV proton beam penetrating the carbon wire of 30 μm diameter, the proton ionization losses of about 35.5 keV completely heat the wire and only 0.67 keV is leaving the wire by the nuclear interaction. So we can assume $\varepsilon_{heat} \approx 1$ (in our previous publications, e. g. [2], we used a smaller value $\varepsilon_{heat} \approx 0.3$ ).

Finally we find the equation that determines the wire oscillation frequency shift depending on the proton beam current $I_p$ penetrating the wire:

$$\frac{\Delta F}{F_0} = -\frac{E}{2\sigma_0}\frac{\alpha\varepsilon_{heat}(\delta_p I_p / e)}{\left[8\lambda S / L + 4\varepsilon\sigma_{ST-B}T_0^3\pi dL + \eta\alpha_{conv}\pi dL\right]}, \tag{9}$$

where $F_0=(1/L)\sqrt{\sigma_0/\rho}$ is the initial frequency of the wire vibrating on the second harmonics, $\sigma_0$ the initial tension of the wire, $\rho$ the density of wire material, $\alpha$ the coefficient of thermal expansion of the wire material, and $E$ the elasticity module of the wire material.

For example, for $E$ = 15 MeV and tungsten wire diameter $d$ = 100 μm we obtain $\delta_p$ = 2.27 MeV. For the proton beam with the Gaussian profile (RMS width of 15 mm) and the average beam current $I_{total}$ = 100 nA, the current deposited into the wire placed at the center of the beam is $I_p = 2.175 \times 10^{-10}$ A (wire length is $L$ = 80 mm). For the loss factor conversion into heat $\varepsilon_{heat}$ = 0.9 and air convection

$\alpha_{conv}$ = 17 W/(m$^2$ K) the temperature increase $\Delta T$ in the wire is 0.8 K and power deposited in the wire is ~0.44 mW (the range of the used monitor parameters is 1.5 × $10^{-6}$–0.15 W). For initial frequency of ~2000 Hz, the frequency shift is ~2.9 Hz.

## 3. VWM DESCRIPTION

The main view of the VWM is presented in Figure 1. The wire (*1*) is stretched between two clips (*4*). The initial tension of the wire defines the frequency of the wire oscillations. The wire is passed through two areas of magnetic fields prepared by pairs of permanent magnets (*2*) covered by magnet poles made from soft iron (*3*). The gap between the magnets is about 1 mm and oscillations occur in the plane of the gap. If the magnetic fields in the gaps are directed in the same direction the first harmonics of the vibrations are generated. In the case of opposite directions the second harmonic is originated. The vibration generation is based on the interaction between electrical current through the wire and magnetic field. The vibrating wire is connected to a positive feedback circuit. The circuit consists of operational amplifiers which amplify oscillation at a certain natural frequency (see [13] for more details).

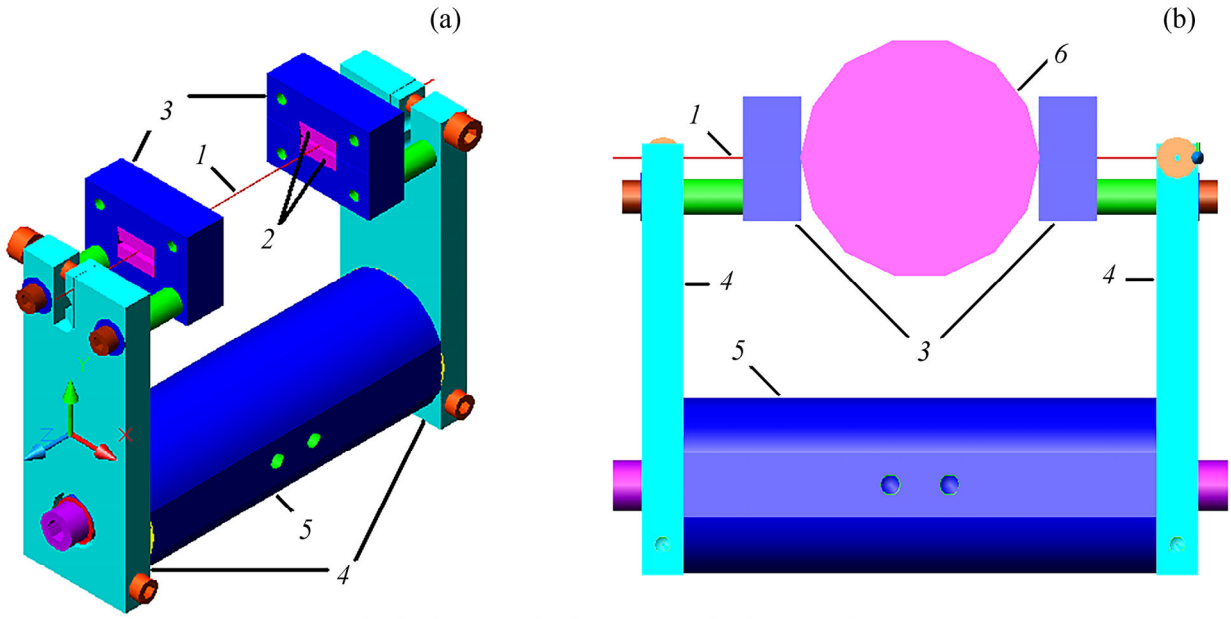


**Fig. 1.** (a) Main view of the monitor with an aperture of 40 mm and a wire length of 80 mm: *1* − vibrating wire, *2* − magnets, *3* − magnet poles, *4* − clamps, *5* − basis. (b) Aperture of the monitor is defined by the circle *6* placed between the magnetic poles.

The VWM can be operated both in the vacuum and in the air. In the vacuum, the level of frequency stability of the signal is less than 0.01 Hz. When the VWM is operating in the air, the fluctuations in the frequency becomes larger because of the convection. The problem is more significant for wires with longer lengths. Figure 2 shows signals of the VWM without any protection against convection (Fig. 2a) and with convection box (Fig. 2b).

The standard error of linear regression of the experimental points in Figure 2a is about 0.4 Hz, and of the experimental points in Figure 2b only 0.0038 Hz, i. e. impact of the box protected from the convection is very essential.

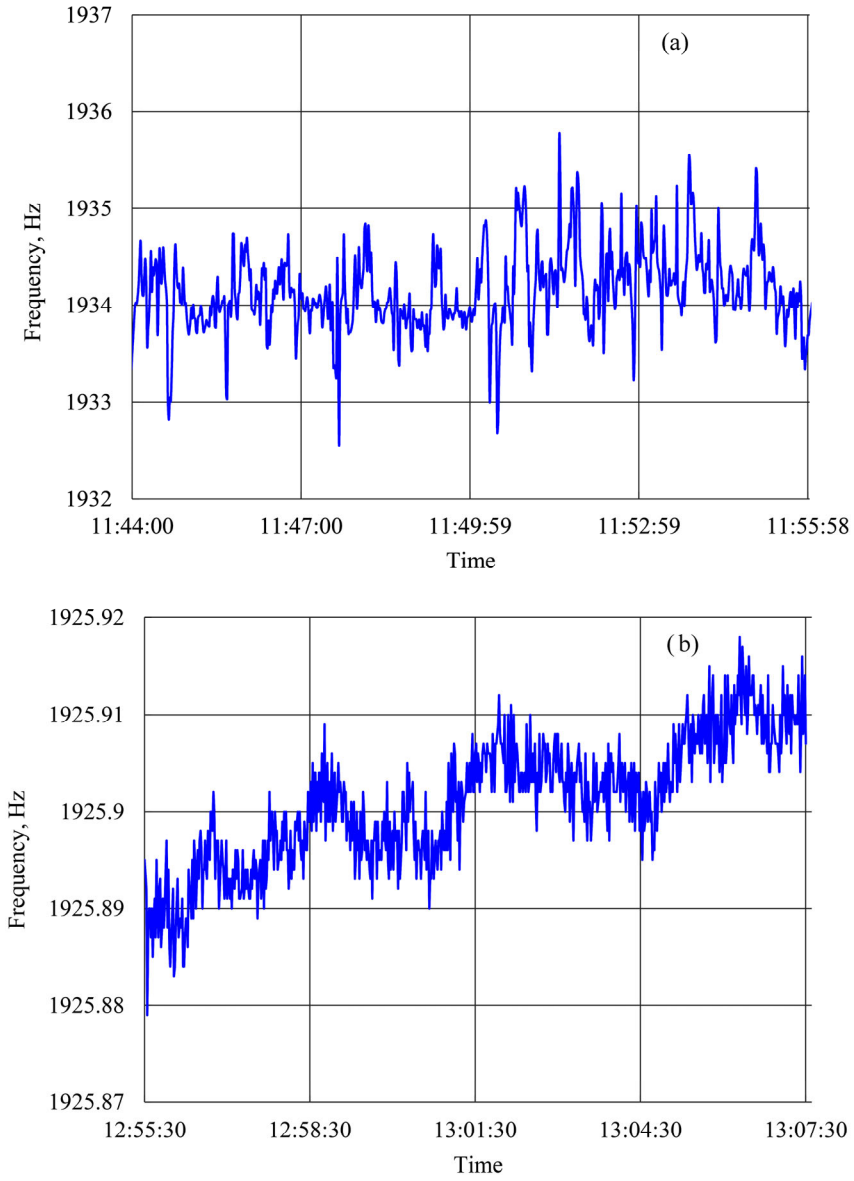


**Fig. 2.** Frequency signal (a) without convection protection and (b) with convection protection.

## 4. EXPERIMENTAL RESULTS

### *4.1. KOMAC AND RADIOCHROMIC FILM TECHNIQUE FOR BEAM PROFILING*

The KOMAC facility consists of a 100 MeV proton linac including a 50 keV ion source, and 20 MeV and 100 MeV beam lines [4]. The project has been designed to deliver a high current or intense proton beam (4.8 mA average beam current for 20 MeV and 1.6 mA for 100 MeV) that can be utilized in either a wide range of R&D fields or various industrial applications [5]. Five 20 MeV beamlines and five 100 MeV beamlines were originally planned. Currently, two of them (TR23 with 30 Hz with 0.6 mA maximum average beam current and 20 MeV energy, and TR103 with 15 Hz with 0.3 mA maximum average beam current and 100 MeV energy) are in operation. Other target rooms will be constructed step

by step in parallel with beam diagnostics instrumentations development and their implementation. In the target room TR23 the beam is extracted from the accelerator vacuum chamber through the titanium foil. For various applications target room is equipped with a 3D movable table with remote control system. Proton beam scattering in air causes the beam to spread out and lose energy, so the beam profile and energy depend on the distance from the vacuum chamber outlet.

For proton beam profile monitoring in air a GAFCHROMIC H-V2 radiochromic dosimetry film is used [14]. This kind of radiochromic films are commonly used for quantitative measurement of absorbed dose of high energy photons [15] and also for dosimetry of a wide range of other radiation sources (electrons, protons, and alpha-particles [16]). Since radiochromic film requires no post-exposure processing, there are no chemicals to dispose of and the film can be handled without other equipment. Dynamic dose range from 10 to 1000 Gy practically without energy dependence, energetic resolution is about 100 keV into the MeV range. The film has high spatial resolution (< 5 μm) and is comprised of a layer containing the active component, marker dye, stabilizers and other components giving the film response. The degree of material coloring depends on the energy imparted to the color producing elements (chromophores) [16].

The radiochromic film has good integral characteristics: < 5% difference in net density for 10 Gy exposures at rates of 3.4 Gy/min and 0.034 Gy/min [14]. After exposure the films were usually scanned

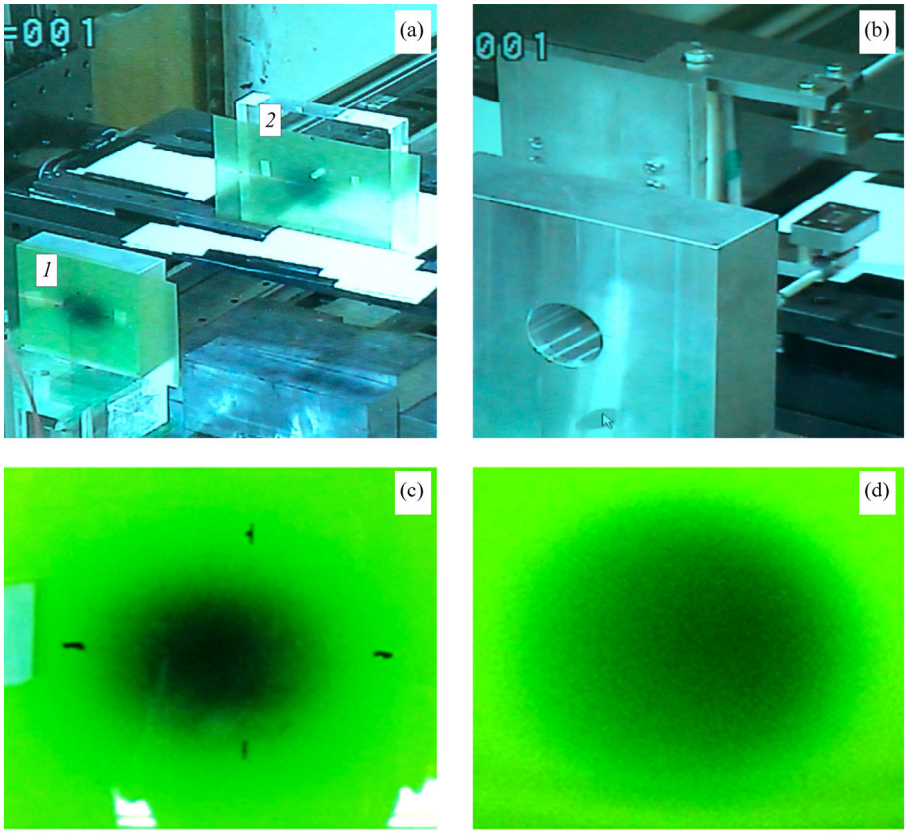


**Fig. 3.** Proton beam profiling by means of GAFCHROMIC film: (a) the collimator made of aluminum (*1*) with thickness 20 mm and 30 mm diameter hole, and plexiglass (*2*) (here will be placed the monitor) are covered by radiochromic film; (b) the close-up view of the aluminum collimator without film (at background the VWM is shown); (c) beam profile on the film mounted on the collimator, and (d) beam profile on the film mounted on the plexiglass.

on special scanner, and then digitalized using image processing program. Figure 3 presents the usage of radiochromic film in our experiment before the VWM installation.

A disadvantage of this technique is that after some quantity of passing particles becomes black and have to be changed. As a complement to the beam profiling by chromic films we suggested to use VWM with improved sensitivity and precision. The choice furthermore is grounded by necessity to measure very low beam current (only $10^{11}$ protons in train instead of nominally expected $1.25 \times 10^{14}$ protons in train).

### *4.2. BEAM PROFILING BY VWM*

The VWM was mounted on the 3D table in the target room TR23 (see Figure 3). The position of the VWM was chosen at 1 m downstream from the extracting window. Initial energy of 20 MeV the protons at this position was decreased to 14.5 MeV.

To protect the magnet system from the protons outside of the wire aperture area (see Figure 1b) the collimator made from Al with 30 mm diameter hole was installed in front of the VWM. Figure 3b presents the collimator and VWM. All components are installed on 3D movable table, which gives us possibility to adjust the vertical position of the VWM and organize the scan of the VWM in the horizontal direction.

Then the VWM was covered by convection protection box. The hole of collimator and beam opening in box were covered by GAFCHROMIC film for aligning of the collimator and VWM on beam line.

The one train of proton beam has 100 μs duration and shots can be repeated only up to 1 Hz repetition rate. Corresponding delay between trains is 1 s and more. This time should be compared with the response time of VWM which is defined by three different heat sink processes (conductivity through the wire, radiation and convection from wire surface). For $L = 80$ mm, $d = 100$ μm, $\varepsilon = 0.3$, and $\alpha_{conv} = 17$ W/(m$^2$ K) the VWM response time is about 2.6 s [17]. At first experiments with 1 Hz repetition rate the frequency response of VWM from consequence trains did not separated from each other and we saw

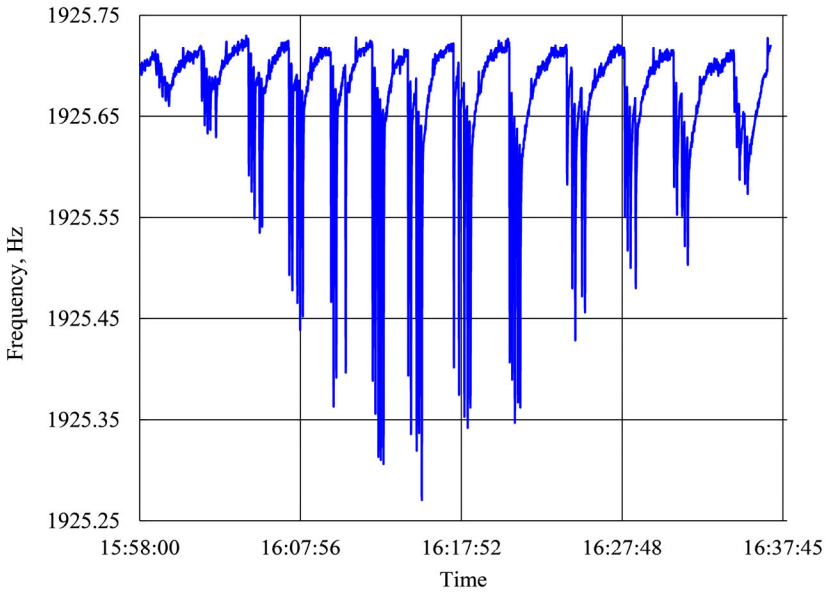


**Fig. 4.** Cumulative measurement data of total scan experiment. One can see that only for positions 2, −18, and −30 mm the beam trains have regular timing structure. The series corresponding to positions −14 mm and −38 mm contain only four proton trains instead of five.

overlapping structure of such trains. For confident separation of trains has been exposed delay between the trains of 10 s (repetition rate 0.1 Hz).

The resulting experiment eventually was made by following scheme: 5 trains with repetition rate 0.1 Hz for fixed transversal positions of the VWM, then delay of 1 min during which VWM position was shifted on 4 mm. The range of positions where we obtained definitive signal from VWM was +2 to −46 mm (totally 13 positions). The result of measurements is presented in Fig. 4 where thirteen measurements in different positions are definitely aggregated.

It is seen from the Figure 4a there is a significant difference between trains in the same transversal position of VWM. The difference can be explained either by the different number into serial trains or transversal shifts of the trains. To clear this question preferable to make experiment with the multi-wire VWM. We suppose that position of trains remain unchangeable and by accumulated data we extract the mean values of frequency drops for trains in fixed position. Figure 5 shows a regular set of the train response for position − 18 mm.

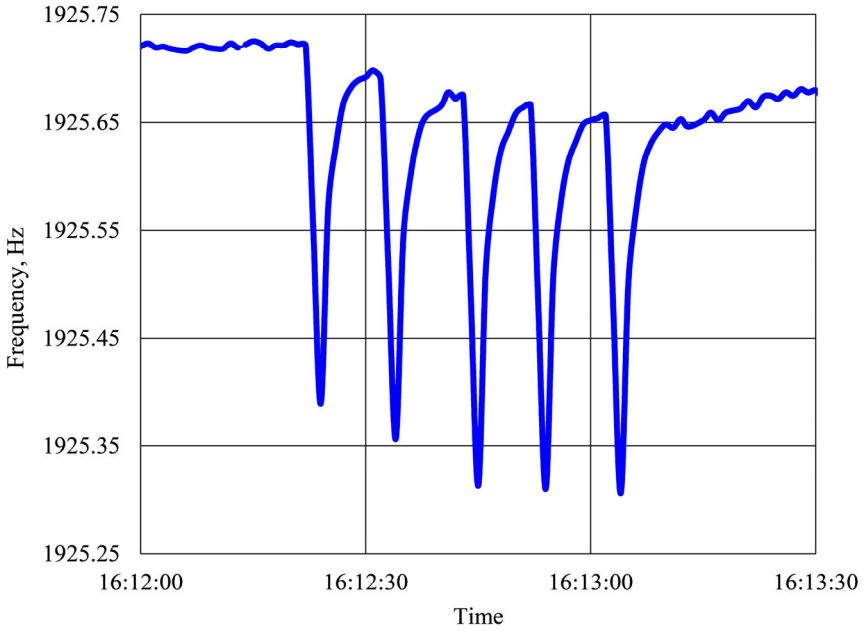


**Fig. 5.** Regular temporal structure of the VWM response of 5 trains in position −18 mm.

It is seen that the abrupt drop of the frequency at train fall on the wire and consequential frequency relaxation to initial value corresponds to typical process of wire heating and further cooling. Such behavior is typical for process of wire heating and further cooling. Since the cooling process is stopped by the next train we also see a small slope of points were the cooling process is terminated. As a numerical value of each train response we calculate the frequency drop at start of heating process to the lowest point. The set of these points for different positions gives the averaging of beam profile at experiment time (see Figure 6).

In the set of measurements corresponding to the position −34 mm one experimental point is removed from calculation. The sets of measurements corresponding to positions −14 mm and −38 mm contain only four proton trains. The fitting of the experimental curve by the Gaussian curve $G\exp(-(x-x_0)^2/2\sigma^2)$ with following parameters: $\sigma$ = 15 mm, $x_0 = -20$ mm, $G = 0.345$ Hz ($x$ is the transversal coordinate).

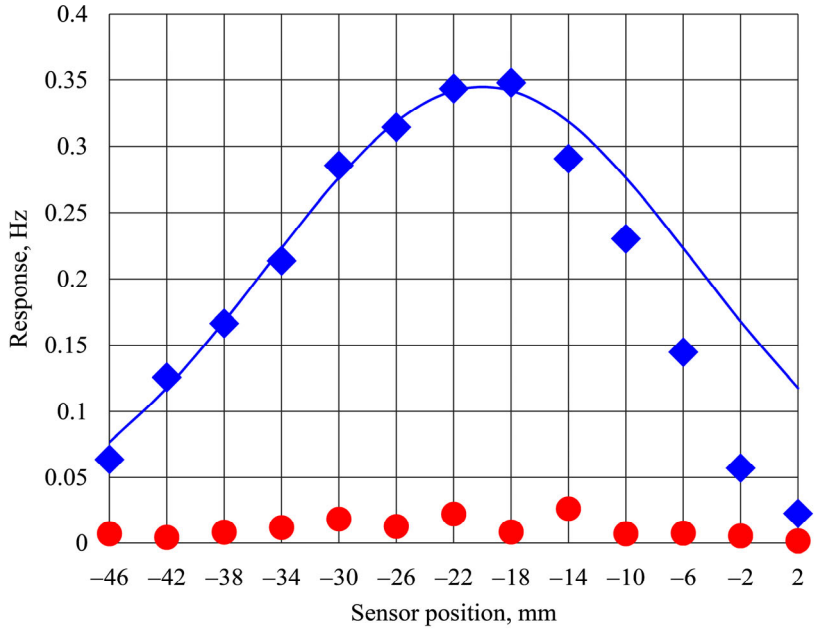


**Fig. 6.** Beam profile, reconstructed by procedure of estimation of frequency drop for each train. Diamonds are the averaging of experimental data at fixed positions of VWM (circles correspond to squares standard deviation by the set of measurements). Solid line is fit of experimental points by the Gaussian curve.

## 5. CONCLUSION

The VWM was applied for profile measurements of the proton beam with very low average current of protons of KOMAC facility. Corresponding frequency shift about 0.5 Hz was sufficient for separate train analysis. This analysis shows the essential difference between serial trains. By measurements in set of the transversal position the proton beam average profile was reconstructed. Due to the large dynamic range of VWM (the maximal frequency deviation up to 1000 Hz) the measurements of proton beam can be provided at higher beam intensities. At KOMAC beam nominal values (e.g., 0.6 mA for TR23) the VWM can be used for beam halo measurements. The important task for further work is the adjusting of the VWM parameters, i. e. definition of coefficient of beam losses to the heat transfer and convection heat losses coefficient for the vibrating wire. Specification of these parameters will allow to use the VWM for absolute measurements. In further experiments it is reasonable also to use the resonance target VWM [13] which allows much more speed of the scan.

## ACKNOWLEDGMENTS

The authors are very thankful to K.-K. Kim, S.-J. Kim, M.-H. Chung, and J.-C. Park for the help in operating the KOMAC facility. The authors are also grateful to R. Reetz and J. Bergoz for many years permanent support. This research was supported by the National Research Foundation of Korea (NRF-2015M2B2A4033273).

## REFERENCES

1. Arutunian, S.G., Avetisyan, A.E., Davtyan, M.M., Harutyunyan, G.S., Vasiniuk, I.E., Chung, M., and Scarpine, V., *Phys. Rev. Spec. Top. – Accel. Beams*, 2014, vol. 17, p. 032802-1.
2. Arutunian, S.G., Mailian, M.R., and Wittenburg, K., *NIM A*, 2007, vol. 572, p. 1022.

3. Decker, G., Arutunian, S., Mailian, M., and Vasiniuk, I., *Beam Instrumentation Workshop*, BIW08, May 4−8, 2008, Lake Tahoe, USA, pp. 36−40.
4. Cho, Y.-S., Kwon, H.-J., Kim, D.-I., Kim, H.-S., Ryu, J.Y., Park, B.-S., Seol, K.T., Song, Y.-G., Yun, S.-P., and Jang, J.-H., *Proc. IPAC2013*, May 12–17, 2013, Shanghai, China, pp. 2052–2054.
5. Kim, K.-R., Kim, K.Y., Cho, Y.-S., Kim, J.-Y., Park, J.-W., and Choi, B.-H., *J. Korean Phys. Soc.*, 2011, vol. 59, p. 521.
6. Nowak, A.-E. and Stein, G., *Feuerfestbau, Werkstoffe-Konstuktion-Ausfuehrung*, Essen: Vulkan-Verlag, 2002.
7. Perkins, D.H., *Introduction to High Energy Physics*, Boston: Addison-Wesley, 1972.
8. Leo, W.R., *Techniques for Nuclear and Particle Physics Experiments*, New York, Berlin, Heidelberg: Springer-Verlag, 1987.
9. Janni, J.F., *Calculations of Energy Loss, Range, Pathlength, Straggling, Multiple Scattering, and the Probability of Inelastic Nuclear Collisions for 0.1 to 1000 MeV Protons*, Tech. Report no. AFWL-TR-65-150, Air Force Weapons Laboratory, New Mexico, 1966.
10. Sternheimer, R.M., Seltzer, S.M., and Berger, M.J., *Phys. Rev. B*, 1982, vol. 26, p. 6067.
11. Elmfors, P., Fasso, A., Huhtinen, M., Lindroos, M., Olsfors, J., and Raich, U., arXiv: physics/9703018v1 [physcs.acc-ph] 12 March 1997.
12. Kumawat, H., Dutta, D., Mantha, V., Mohanty, A.K., Satyamurthy, P., Choudhury, R.K., and Kailas, S., *NIM B*, 2008, vol. 266, p. 604.
13. Arutunian, S.G., Chung, M., Harutyunyan, G.S., Margaryan, A.V., Lazareva, E.G., Lazarev, L.M., and Shahinyan, L.A., *Rev. Sci. Instrum.*, 2016, vol. 87, p. 023108.
14. http://www.gafchromic.com/documents/gafchromic-hdv2.pdf
15. Chen, S.N., Gauthier, M., Bazalova-Carter, M., Bolanos, S., Glenzer, S., Riquier, R., Revet, G., Antici, P., Morabito, A., Propp, A., Starodubstev, M., and Fuchs, J., *Absolute Dosimetric Characterization of Gafchromic EBT3 and HDv2 Films Using Commercial Flat-Bed Scanners and Evaluation of the Scanner Response Function Variability*. http://waset.org/publications/16486/characterization-of-hd-v2-gafchromic-film-for-measurement-of-spatial-dose-distribution-from-alpha-particle-of-5.5-mev
16. Kalef-Ezra, J., *Radiochromic Film Dosimetry*, www.efie.gr/index.php/gr/
17. Arutunian, S.G., Choe, D., Chung, M., Harutyunyan, G.S., Margaryan, A.V., and Lazareva, E.G., *Proc. 25th Annual Int*. Laser Physics Workshop 2016, July 11−15, 2016, Yerevan, Armenia (will be published).